Electronic Supporting Information

Peraurated Nickel Carbide Carbonyl Clusters: the Cationic $[Ni_6(C)(CO)_8(AuPPh_3)_8]^{2+}$ Monocarbide and the $[Ni_{12}(C)(C_2)(CO)_{17}(AuPPh_3)_3]^{-}$ Anion Containing one Carbide and one Acetylide Unit.

Marco Bortoluzzi,[a] Iacopo Ciabatti,[b] Cristina Femoni,[b] Mohammad Hayatifar,[b] Maria Carmela Iapalucci,[b] Giuliano Longoni [b] and Stefano Zacchini[b]*

[a] *Dipartimento di Scienze Molecolari e Nanosistemi, Ca' Foscari University of Venice, Dorsoduro 2137 – 30123 Venezia, Italy*

[b] *Dipartimento di Chimica Industriale "Toso Montanari", Università di Bologna, Viale Risorgimento 4 - 40136 Bologna, Italy.*

Table S.1.

Main bonding distances (Å) of $[Ni_6(C)(CO)_8(AuPPh_3)_8]^{2+}$.

	Range	**Average**
Ni_{eq}-Ni_{eq}	2.656(3)	
Ni_{eq}-Ni_{ap}	2.508(3)-2.922(3)	2.715(4)
Ni_{eq}-C	1.857(2)	
Ni_{ap}-C	1.992(3)	
Ni_{eq}-Au	2.601(2)-2.656(2)	2.626(4)
Ni_{ap}-Au	2.8561(8)	
$Ni_{ap}\cdots$Au	3.404(1)	
Au-Au	2.8291(10)	
Au-P	2.285(5)-2.292(5)	2.288(7)

Table S.2.

Main bonding distances (Å) of $[Ni_{12}(C)(C_2)(CO)_{17}(AuPPh_3)_3]^{-}$.

	Range	**Average**
Ni-Ni	2.4110(14)-3.053(3)	2.626(7)
Ni-Au	2.5884(10)-2.9185(11)	2.746(4)
Ni-(C_2)	1.953(7)-2.217(7)	2.09(2)
Ni(2)···C(2)	2.386(7)	
Ni(2)···C(3)	2.391(7)	
Ni-C	1.905(7)-1.938(7)	1.922(16)
Au-C	2.139(7)	2.139(7)
Au-P	2.281(2)-2.2883(19)	2.286(3)
Ni(10)···Ni(2)	3.743(2)	
Ni(2)···Au(1)	4.005(1)	
Ni(6)···Ni(7)	3.355(3)	
C(1)···C(2)	2.781(11)	
C(1)···C(3)	2.798(11)	

Table S.3.

HOMO-LUMO gap (eV) computed at DFT M06 level for the model system $[Ni_6(C)(CO)_8(AuPH_3)_8]^{2+}$.

	HOMO-LUMO gap (eV)
M06/LANL2MB	3.07
M06/LANL2DZ	3.18
M06/SBKJC	3.07

Table S.4.

Mulliken charge distribution on carbon atoms (a.u.) for the model system $[Ni_6(C)(CO)_8(AuPH_3)_8]^{2+}$.

	Mulliken charges (a.u.)	
	carbide	C (CO)
M06/LANL2MB	-0.091	0.320 --- 0.378
M06/LANL2DZ	-0.673	0.283 --- 0.319

M06/SBKJC	-0.845	-0.187 --- 0.143

Table S.5.

HOMO-LUMO gap (eV) computed at DFT M06 and EDF2 levels for the model system $[Ni_{12}(C)(C_2)(CO)_{17}(AuPH_3)_3]^-$.

	HOMO-LUMO gap (eV)
M06/LANL2MB	2.08 (a)
M06/LANL2DZ	2.29 (b)
M06/6-31G(d,p)+LANL2TZ(f)	2.28
M06/SBKJC	2.35
EDF2/LACVP**	1.80 (c)

(a) The computed value for the optimised geometry is 1.95 eV. (b) The computed value for the optimised geometry is 2.32 eV. (c) The computed value for $[Ni_{12}(C)(C_2)(CO)_{17}(AuPPh_3)_3]^-$ is 1.81 a.u.

Table S.6.

Mulliken charge distribution on carbon atoms (a.u.) for the model system $[Ni_{12}(C)(C_2)(CO)_{17}(AuPH_3)_3]^-$.

	Mulliken charges (a.u.)		
	acetylide	carbide	C (CO)
M06/LANL2MB	-0.094 / -0.086 (d)	-0.093 (e)	0.251 --- 0.333 (f)
M06/LANL2DZ	-0.527 / -0.420 (g)	-1.147 (h)	0.097 --- 0.307 (i)
M06/6-31G(d,p)+LANL2TZ(f)	-0.311 / -0.264	-0.763	0.307 --- 0.508
M06/SBKJC	-0.724 / -0.712	-0.782	-0.226 --- -0.096
EDF2/LACVP**	-0.631 / -0.605 (j)	-0.831 (k)	0.191 --- -0.441 (l)

Optimised geometry: (d) -0.033 / -0.013; (e) -0.082; (f) 0.250 --- 0.330. Optimised geometry: (g) -0.475 / -0.407; (h) -1.343; (i) 0.103 --- 0.264. $[Ni_{12}(C)(C_2)(CO)_{17}(AuPPh_3)_3]^-$: (j) -0.636 / -0.610; (k) -0.830; (l) 0.166 --- 0.472.

Table S.7.

Electron density (a.u). at the middle of C-C distances in $[Ni_{12}(C)(C_2)(CO)_{17}(AuPH_3)_3]^-$.

	Electron density at the middle of C-C distances (a.u.)	
	acetylide	acetylide-carbide
M06/LANL2MB	0.29 (m)	0.03 / 0.03 (n)
M06/LANL2DZ	0.28 (n)	0.03 / 0.03 (n)
M06/6-31G(d,p)+LANL2TZ(f)	0.29	0.03 / 0.03
M06/SBKJC	0.28	0.03 / 0.03
EDF2/LACVP**	0.30 (o, p)	0.03 / 0.03 (p)

(m) 0.28 for the optimised structure. (n) The same values for the optimised structure. (o) For comparison: 0.40 acetylene, 0.34 ethylene, 0.24 ethane. (p) The same values for $[Ni_{12}(C)(C_2)(CO)_{17}(AuPPh_3)_3]^-$.

Table S.8.

Selected computed bond orders for $[Ni_{12}(C)(C_2)(CO)_{17}(AuPH_3)_3]^-$.

	Bond orders	
	acetylide	CO
M06/LANL2MB (q)	1.30	2.15 --- 2.34
M06/LANL2DZ (q)	1.25	2.09 --- 2.19
M06/6-31G(d,p)+LANL2TZ(f) (q)	1.16	1.93 --- 2.10
M06/SBKJC (q)	1.84	2.35 --- 2.51
EDF2/LACVP** (r)	1.27	2.37 --- 2.62

(q) Mulliken analysis. (r) Löwdin analysis.

Figure S.1.

MO energy diagram (eV) for the model system $[Ni_6(C)(CO)_8(AuPH_3)_8]^{2+}$ *(M06/LANL2DZ calculations).*

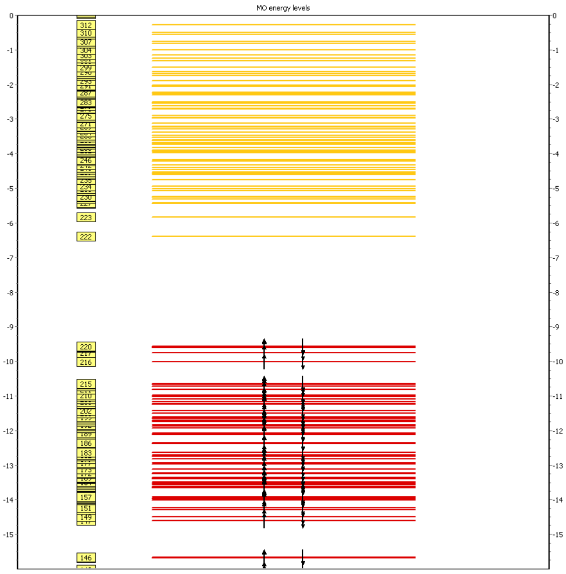

Figure S.2.

HOMO of $[Ni_6(C)(CO)_8(AuPH_3)_8]^{2+}$ *(surface isovalue = 0.055 a.u., M06/LANL2DZ calculations).*

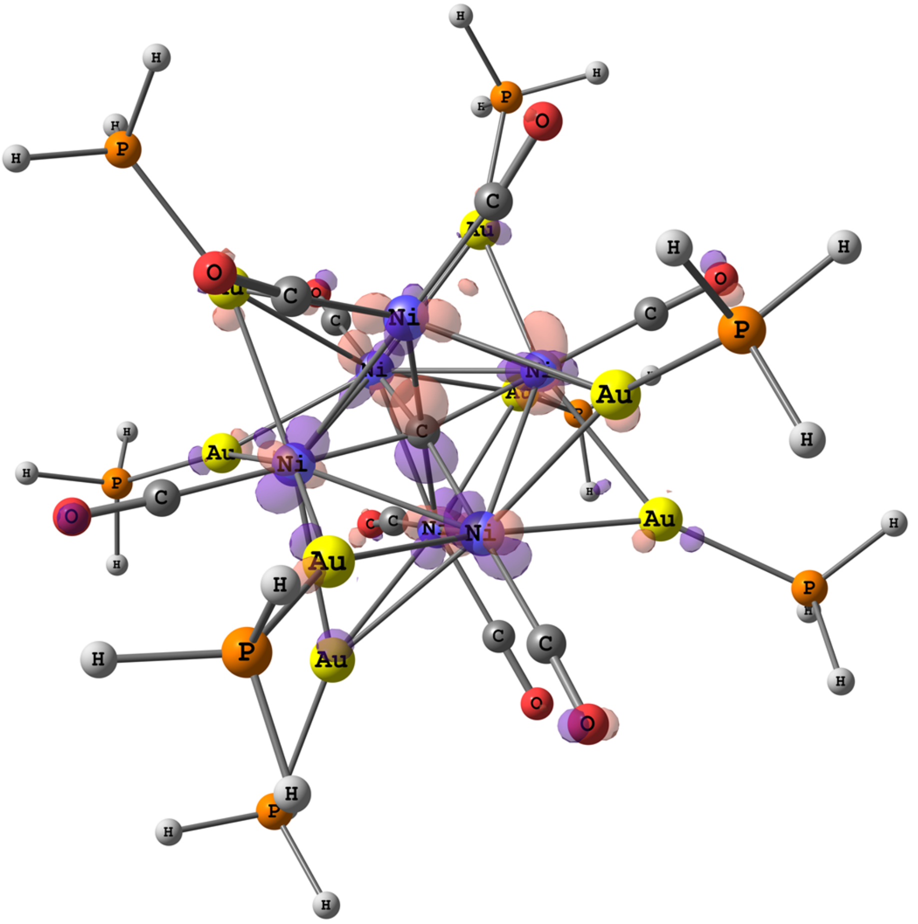

Figure S.3.

MO energy diagram (eV) for the model system $[Ni_{12}(C)(C_2)(CO)_{17}(AuPH_3)_3]^{-}$ *(M06/6-31G(d,p)+LANL2TZ(f) calculations).*

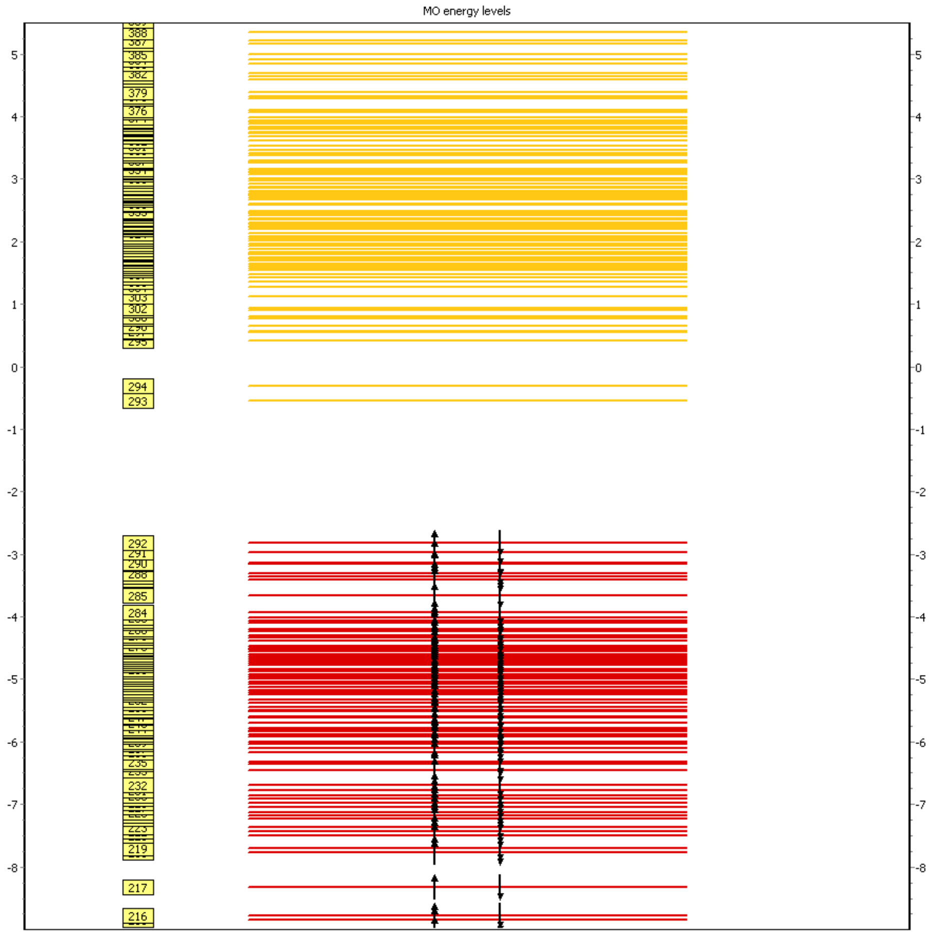

Figure S.4.

HOMO-75, HOMO-76 and HOMO-77 of $[Ni_{12}(C)(C_2)(CO)_{17}(AuPH_3)_3]^{-}$ *(surface isovalue = 0.05 a.u., M06/6-31G(d,p)+LANL2TZ(f) calculations).*

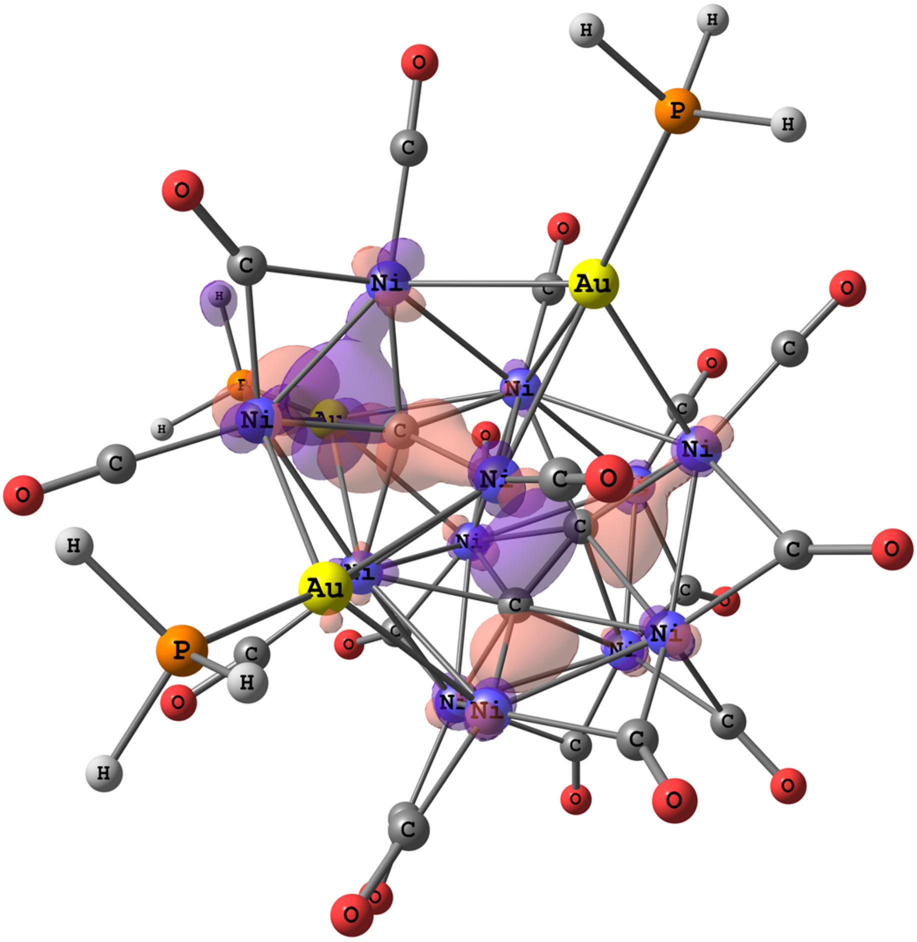

HOMO-75

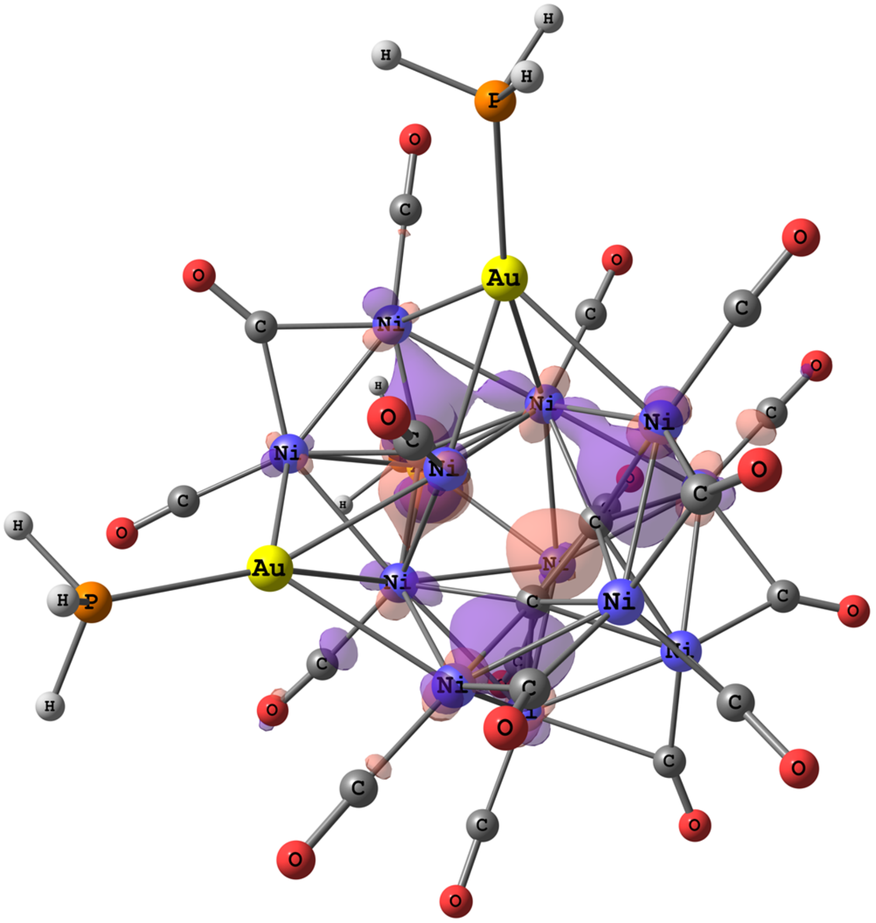

HOMO-76

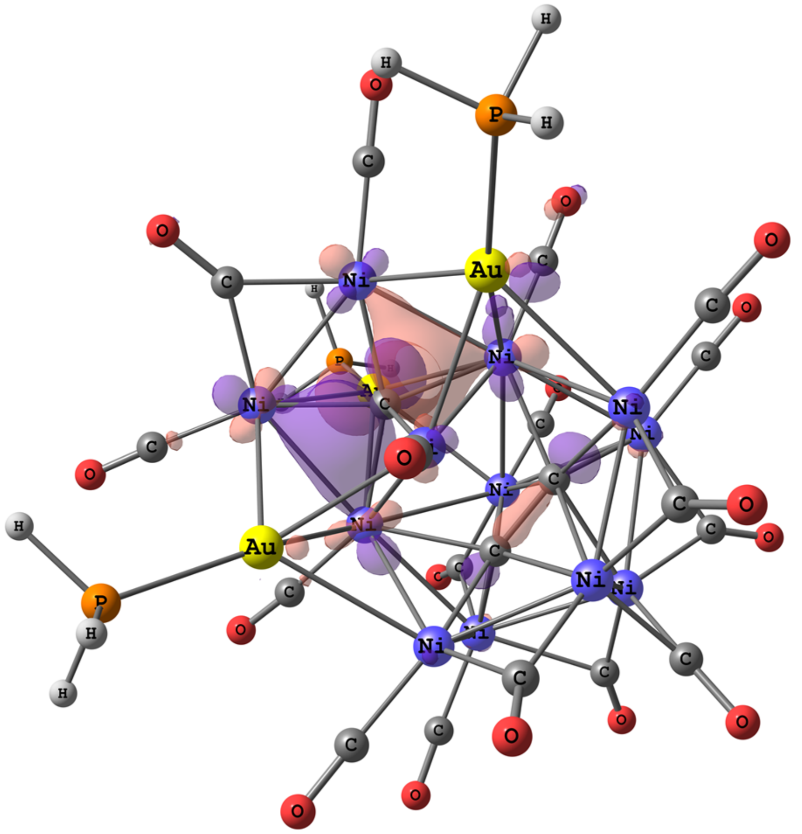

HOMO-77

General experimental procedures

All reactions and sample manipulations were carried out using standard Schlenk techniques under nitrogen and in dried solvents. All the reagents were commercial products (Aldrich) of the highest purity available and used as received, except $[NEt_4]_2[Ni_9(C)(CO)_{17}]$,[1] $[NEt_4]_2[Ni_{10}(C_2)(CO)_{15}]$,[2] $Ni_6(C)(CO)_9(AuPPh_3)_4$ [3] and $Au(PPh_3)Cl$ [4] which have been prepared according to the literature. Analyses of Ni and Au were performed by atomic absorption on a Pye-Unicam instrument. Analyses of C, H and N were obtained with a Thermo Quest FlashEA 1112NC instrument. IR spectra were recorded on a Perkin Elmer Spectrum One interferometer in CaF_2 cells. $^{31}P\{^1H\}$ NMR measurements were performed on a Varian Mercury Plus 400 MHz instrument. The phosphorous chemical shifts were referenced to external H_3PO_4 (85% in D_2O). Structure drawings have been performed with SCHAKAL99.[5]

Synthesis of $[Ni_6(C)(CO)_8(AuPPh_3)_8][BF_4]_2$ ([1][BF$_4$]$_2$)

$HBF_4 \cdot Et_2O$ (158 μL, 1.16 mmol) was added drop-wise to a solution of $Ni_6(C)(CO)_9(AuPPh_3)_4$ (0.580 g, 0.236 mmol) in CH_2Cl_2 (20 mL), and the resulting mixture stirred at room temperature for 4 h. The solvent was removed *in vacuo* and the residue washed with water (40 mL), and extracted in CH_2Cl_2 (20 mL). Crystals of $[Ni_6(C)(CO)_8(AuPPh_3)_8][BF_4]_2$ suitable for X-ray analysis were obtained by slow diffusion of n-hexane (40 mL) on the CH_2Cl_2 solution (yield 0.210 g, 20% based on Ni, 40% based on Au).

$C_{153}H_{120}Au_8B_2F_8Ni_6O_8P_8$ (4435.86): calcd. C 41.44, H 2.73, Ni 7.85, Au 35.57; found: C 41.21, H 2.95, Ni 7.59, Au 35.88.

IR (nujol, 293 K) ν(CO): 1977(s), 1847(w), 1638(w) cm^{-1}. IR (CH_2Cl_2, 293 K) ν(CO): 2000(m), 1979(s), 1862(w), 1773(w) cm^{-1}.

$^{31}P\{^1H\}$ NMR (CD_2Cl_2, 298 K) δ (ppm): 56.4 (s). $^{31}P\{^1H\}$ NMR (CD_2Cl_2, 203 K) δ (ppm): 55.0 (s).

Synthesis of $[NEt_4][Ni_{12}(C)(C_2)(CO)_{17}(AuPPh_3)_3] \cdot thf$ ([NEt$_4$][2]·thf)

$Au(PPh_3)Cl$ (1.05 g, 2.10 mmol) was added as a solid to a solution of $[NEt_4]_2[Ni_9(C)(CO)_{17}]$ (0.894 g, 0.700 mmol) and $[NEt_4]_2[Ni_{10}(C_2)(CO)_{15}]$ (0.910 g, 0.700 mmol) in thf (20 mL), and the resulting mixture stirred at room temperature for 6 h. The solvent was removed *in vacuo* and the residue washed with water (40 mL), and extracted in thf (20 mL). Crystals of $[NEt_4][Ni_{12}(C)(C_2)(CO)_{17}(AuPPh_3)_3] \cdot thf$ suitable for X-ray analysis were obtained by slow diffusion of n-hexane (40 mL) on the thf solution (yield 0.611 g, 20% based on Ni, 31% based on Au).

$C_{86}H_{73}Au_3NNi_{12}O_{18}P_3$ (2796.78): calcd. C 37.04, H 2.64, N 0.50, Ni 24.95, Au 21.21; found: C 36.85, H 2.92, N 0.84, Ni 25.12, Au 21.06.

IR (nujol, 293 K) ν(CO): 2002(s), 1971(sh), 1938(m), 1824(m) cm^{-1}. IR (thf, 293 K) ν(CO): 2009(s), 1975(m), 1945(sh), 1888(w), 1832(w) cm^{-1}.

$^{31}P\{^1H\}$ NMR (d^8-thf, 298 K) δ (ppm): 49.0 (s, 2P), 48.2 (s, 1P).

X-ray Crystallographic Study.

Crystal data and collection details for $[Ni_6(C)(CO)_8(AuPPh_3)_8][BF_4]_2$ and $[NEt_4][Ni_{12}(C)(C_2)(CO)_{17}(AuPPh_3)_3]$·thf are reported in Table S.9. The diffraction experiments were carried out on a Bruker APEX II diffractometer equipped with a CCD detector using Mo–Kα radiation. Data were corrected for Lorentz polarization and absorption effects (empirical absorption correction SADABS).[6] Structures were solved by direct methods and refined by full-matrix least-squares based on all data using F^2.[7] Hydrogen atoms were fixed at calculated positions and refined by a riding model. All non-hydrogen atoms were refined with anisotropic displacement parameters, unless otherwise stated.

$[Ni_6(C)(CO)_8(AuPPh_3)_8][BF_4]_2$: The asymmetric unit of the unit cell contains one fourth of a cluster cation (located on $\bar{4}$) and one half of a $[BF_4]^-$ anion disordered over four positions two by two related by a 2-fold axis. The two independent images of these anions have been refined isotropically using one occupancy parameter per disordered group. The C-atoms of the Ph-rings were constrained to fit regular hexagons (AFIX 66 line in SHELXL). Similar *U* restraints were applied to the C-atoms of the Ph-rings (s.u. 0.01). The $[BF_4]^-$ anions have been restrained to have similar geometries (SAME line in SHELXL, s.u. 0.02) and similar *U* parameters (SIMU line in SHELXL, s.u. 0.01). Restraints to bond distances were applied as follow (s.u. 0.02): 1.37 Å for B–F in $[BF_4]^-$.

$[NEt_4][Ni_{12}(C)(C_2)(CO)_{17}(AuPPh_3)_3]$·thf: The asymmetric unit of the unit cell contains one cluster anion, one $[NEt_4]^+$ cation and one thf molecule (all located on general positions). The C-atoms of the Ph-rings were constrained to fit regular hexagons (AFIX 66 line in SHELXL). One Ph ring is disordered over two positions and, therefore, it has been split and refined using one occupancy parameter per disordered group. Similar *U* restraints were applied to the $[NEt_4]^+$ cation (s.u. 0.01) and, moreover, its atoms have been restrained to isotropic behaviour (ISOR line in SHELXL, s.u. 0.01). Similar *U* restraints were applied to the thf molecule (s.u. 0.01). Restraints to bond distances were applied as follow (s.u. 0.01): 1.47 Å for C–N and 1.53 Å for C–C in $[NEt_4]^+$; 1.43 Å for C–O and 1.53 Å for C–C in thf.

Table S.9.

Crystal data and experimental details for $[Ni_6(C)(CO)_8(AuPPh_3)_8][BF_4]_2$ *and* $[NEt_4][Ni_{12}(C)(C_2)(CO)_{17}(AuPPh_3)_3]\cdot thf$*.*

	$[Ni_6(C)(CO)_8(AuPPh_3)_8][BF_4]_2$	$[NEt_4][Ni_{12}(C)(C_2)(CO)_{17}(AuPPh_3)_3]\cdot thf$
Formula	$C_{153}H_{120}Au_8B_2F_8Ni_6O_8P_8$	$C_{86}H_{73}Au_3NNi_{12}O_{18}P_3$
Fw	4435.86	2796.78
T, K	100(2)	100(2)
λ, Å	0.71073	0.71073
Crystal system	Tetragonal	Monoclinic
Space Group	*P*4$_2$/*n*	*C*2/*c*
a, Å	23.337(3)	24.132(4)
b, Å	23.337(3)	15.619(3)
c, Å	14.2514(18)	48.350(8)
β, °	90	97.681(2)
Cell Volume, Å^3	7761.3(17)	18060(5)
Z	2	8
D_c, g cm^{-3}	1.898	2.057
μ, mm^{-1}	8.381	7.407
F(000)	4208	10864
Crystal size, mm	0.16×0.13×0.10	0.18×0.16×0.12
θ limits, °	1.23–25.03	1.56–25.03
Index ranges	$-27 \leq h \leq 27$ $-27 \leq k \leq 27$ $-15 \leq l \leq 16$	$-28 \leq h \leq 28$ $-18 \leq k \leq 18$ $-57 \leq l \leq 57$
Reflections collected	54146	85012

Independent reflections	6843 [R_{int} = 0.2047]	15948 [R_{int} = 0.0436]
Completeness to θ max	99.9%	99.9%
Data / restraints / parameters	6843 / 296 / 382	15948 / 401 / 1018
Goodness on fit on F^2	1.005	1.064
R_1 ($I > 2\sigma(I)$)	0.0619	0.0412
wR_2 (all data)	0.1726	0.1004
Largest diff. peak and hole, e Å^{-3}	2.463 / –1.184	2.906 / –1.586

CCDC 1005642-1005643 contain the supplementary crystallographic data for this paper. These data can be obtained free of charge at www.ccdc.cam.ac.uk/conts/retrieving.html [or from the Cambridge Crystallographic Data Centre, 12, Union Road, Cambridge CB2 1EZ, UK; fax: (internat.) +44-1223/336-033; E-mail: deposit@ccdc.cam.ac.uk].

Computational details

The electronic structures of the clusters were investigated at DFT level without symmetry constrains, using the hyper-GGA M06 functional [8] in combination with several ECP-based basis sets (LANL2MB, LANL2DZ,[9] SBKJC,[10] and 6-31G(d,p)+LANL2TZ(f) on the metal centres).[11] Further calculations were performed with the hybrid DFT functional EDF2 [12] and the LACVP** basis set.[13] Single-point calculations were carried out on the model systems $[Ni_{12}(C_2)(C)(CO)_{17}(AuPH_3)_3]^-$ and $[Ni_6(C)(CO)_8(AuPH_3)_8]^{2+}$, which were obtained from the X-Ray data by removing the counter-ions and the solvent molecules and by replacing the phenyl rings with hydrogen atoms. In order to ascertain the influence of the substituents on the phosphine ligands, a single-point calculation at EDF2/LACVP** level was made also for the anion $[Ni_{12}(C)(C_2)(CO)_{17}(AuPPh_3)_3]^-$. Finally, the geometry optimisation of $[Ni_{12}(C)(C_2)(CO)_{17}(AuPH_3)_3]^-$ was carried out at M06/LANL2MB and M06/LANL2DZ levels. The software used for M06 calculations was Gaussian 09,[14] while Spartan 08 [15] was used for EDF2 calculations. All the structures are reported as supplementary .xyz files for clarity.

References

(1) A. Ceriotti, G. Longoni, M. Manassero, M. Perego and M. Sansoni, *Inorg. Chem.,* 1985, **24**, 117.

(2) A. Ceriotti, G. Longoni, M. Manassero, N. Masciocchi, L. Resconi and M. Sansoni, *Chem. Commun.,* 1985, 181.

(3) I. Ciabatti, C. Femoni, M. C. Iapalucci, A. Ienco, G. Longoni, G. Manca and S. Zacchini, *Inorg. Chem.,* 2013, **52**, 10559.

(4) C. Kowala and J. M. Swan, *Aust. J. Chem.,* 1966, **19**, 547.

(5) E. Keller, SCHAKAL99, University of Freiburg, Germany, 1999.

(6) G. M. Sheldrick, *SADABS*, Program for empirical absorption correction, University of Göttingen, Germany, 1996.

(7) G. M. Sheldrick, *SHELX97*, Program for crystal structure determination, University of Göttingen, Germany, 1997.

(8) Y. Zhao and D. G. Truhlar, *Theor. Chem. Acc.,* 2008, **120**, 215.

(9) (a) P. J. Hay and W. R. Wadt, *J. Chem. Phys.,* 1985, **82,** 270; (b) W. R. Wadt and P. J. Hay, *J. Chem. Phys.,* 1985, **82**, 284; (c) P. J. Hay and W. R. Wadt, *J. Chem. Phys.,* 1985, **82**, 299.

(10) (a) W. J. Stevens, H. Basch and M. Krauss, *J. Chem. Phys.,* 1984, **81**, 6026; (b) W. J. Stevens, M. Krauss, H. Basch and P. G. Jasien, *Can. J. Chem.,* 1992, **70**, 612.

(11) (a) M. M. Francl, W. J. Pietro, W. J. Hehre, J. S. Binkley, D. J. DeFrees, J. A. Pople and M. S. Gordon, *J. Chem. Phys.,* 1982, **77**, 3654; (b) L. E. Roy, P. J. Hay and R. L. Martin, *J. Chem. Theory Comput.,* 2008, **4**, 1029.

(12) C. Y. Lin, M. W. George and P. M. Gill, W. *Aust. J. Chem.,* 2004, **57**, 365.

(13) (a) W. J. Hehre, R. Ditchfield and J. A. Pople, *J. Chem. Phys.,* 1972, **56**, 2257; (b) P. J. Hay and W. R. Wadt, *J. Chem. Phys.,* 1985, **82**, 270; (c) M. Dolg, in “Modern Methods and Algorithms of Quantum Chemistry” (Grotendorst, J. ed.), John Neumann Institute for Computing, NIC Series, Jülich, 2000, vol. 1, pp. 479–508.

(14) *Gaussian 09*, Revision C.01, M. J. Frisch, et al., Gaussian, Inc., Wallingford CT, 2010.

(15) *Spartan ’08*, version 1.1.1, Wavefunction, Inc., Irvine CA, 2009. Except for molecular mechanics and semi-empirical models, the calculation methods used in Spartan have been documented in: Y. Shao, et al. *Phys. Chem. Chem. Phys.,* 2006, **8**, 3172.